Temporal G-Neighbor Filtering for Analog Domain Noise Reduction in Astronomical Videos

Kamilla Aliakhmet, *Student Member, IEEE*, and Alex Pappachen James, *Senior Member, IEEE*

***Abstract*—Astronomical images obtained from existing cameras are subjected to various types of noise artifacts. Impulse noise is one of them and it is visible as dark and bright spots on the image. Common practice to remove impulse noise is to perform averaging of several frames. This will increase signal-to-noise ratio of the image, however, impulse noise might still be present. The noisy image will hinder the performance of further processing operations such as edge detection. In this brief, variable pixel G-neighbor temporal filtering circuit is proposed to improve the quality of astronomical images with the impulse noise. As compared to conventional averaging of frames in the time domain, where all pixels are summed, the proposed circuit select pixels in each frame that are closest to the reference pixel. The circuit operates in the analog domain, and it was designed and tested using 180-nm CMOS technology. Simulations demonstrate improvement in the peak-signal-to-noise (PSNR) ratio, mean-squared-error (MSE) and structural similarity index measure (SSIM) as compared to conventional averaging of frames.**

***Index Terms*—Temporal filtering, denoising, astronomical images, edge detection.**

I. Introduction

IMAGES of astronomical objects tend to be severely corrupted by noises from various sources. One of the common noise types is the impulse noise, which can originate from thermal generations in pixel [1], or cosmic array hitting the sensor [2]. There are a number of algorithms proposed to remove impulse noise from astronomical images [3]. Many of them, however, are implemented in the digital domain. Conversion of an analog input signal into digital format can cause additional delays due to complex circuitry and errors from quantization [4]. In this brief, we focus on designing an analog pre-processing unit that can be built into the pixel sensor of a telescope camera.

To retrieve information from a continuous noisy image sequence, the simplest method is to average several frames. All the pixels are given the same weights, thus it is a simple arithmetic mean operation within the fixed window. For time-varying noise, this might require processing of a large number of frames to significantly improve signal-to-noise ratio of the images. Implementation of temporal mean filter that can process thousands of image sequences requires large number of circuit components. This is not practical for applications where processing is carried out within the pixel.

A new method is proposed in this brief to improve the performance of the temporal mean filter without the cost of increasing the required chip area. Instead of considering all pixels in the window, pixels with similar intensities (G-neighbor) are selected for processing in the analog domain. Hardware performance is evaluated for aspects such as processing time, total area and power consumption.

Manuscript received February 23, 2019; accepted March 25, 2019. Date of publication March 27, 2019; date of current version April 30, 2019. This brief was recommended by Associate Editor N. M. Neihart. *(Corresponding author: Alex Pappachen James.)*

K. Aliakhmet is with the Circuits and Systems Group, School of Engineering, Nazarbayev University, Astana 010000, Kazakhstan.

A. P. James is with the Department of Electrical and Computer Engineering, School of Engineering, Nazarbayev University, Astana 010000, Kazakhstan (e-mail: apj@ieee.org).

Color versions of one or more of the figures in this paper are available online at http://ieeexplore.ieee.org.

Digital Object Identifier 10.1109/TCSII.2019.2907817

II. Methodology

A. Temporal G-Neighbor Selection

The concept of G-neighbors is first proposed in [5], where pixels are processed based not on their physical proximity, but their similarity in terms of their intensities. G-neighbor filter has been proposed for denoising applications, where real-time hardware processing of the image is desired. Generalized neighbors or G-neighbors are selected on the condition that pixels satisfy certain criteria. Suppose the values of pixel P1 and pixel P2 are A and B, respectively. The simplest model to consider is that P1 and P2 are G-neighbors only if $|A-B| < \eta$, the absolute difference between pixel intensities, is smaller than predefined threshold η. Similarly, other criteria can be applied for denoising of images with multiplicative noise models: $|A-B|/(A+B) < \eta$. The general format of neighborhood criteria can therefore be extended to the format given in (1).

$$NEIGH(A,B) = g(|A-B|) < \eta \tag{1}$$

where, function $g(|A-B|)$ depends on the difference of intensities between two pixels and η is a threshold value. In G-neighbor filtering, instead of processing all pixels in the window, the algorithm selects pixels that are "neighbors" to the reference pixel. This modification is performed by applying similarity mask on the image along with weights of the filter of interest.

In denoising of image sequences, a similar technique is applied to the continuous signal arriving at each pixel. In Fig. 1a, the sequence of five images is presented. Processing is carried out on each pixel separately in a parallel manner. In Fig. 1b, we demonstrate G-neighbor temporal filtering on a

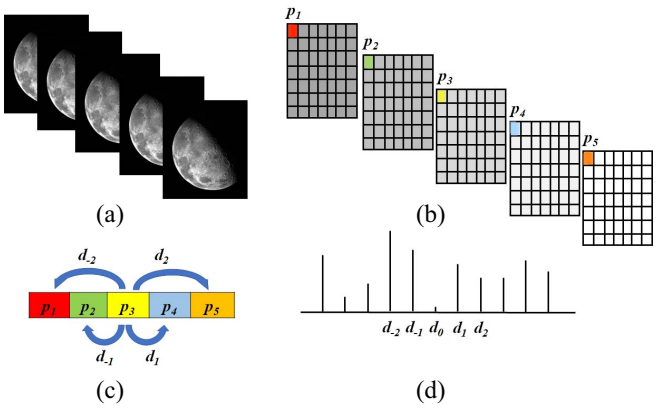

Fig. 1. G-neighbor temporal filtering: (a) video frames, (b) pixel on each frame is selected, (c) intensity values for five frames are saved, (d) the distance between frame of interest and reference frame is calculated.

single pixel over a period of time. Initially, the values of pixel intensities for five consecutive frames p_1, p_2, p_3, p_4, p_5 are stored as demonstrated in Fig. 1c. Then, the distance between each value of p_i and the reference frame are calculated. They are denoted as d_{-2}, d_{-1}, d_0, d_1, d_2 in Fig. 1d. The reference frame is selected to be $(N+1)/2$ for N frames.

Finally, to select G-neighbor pixel, thresholding operation is applied on the distance between pixel on each frame and the reference pixel according to (2). The value of threshold η can be found experimentally.

$$S_G = \begin{cases} 1, & \text{if } |d_k| \le \eta \\ 0, & \text{otherwise,} \end{cases} \tag{2}$$

where, S_G denotes similarity mask and d_k is difference in the intensities between two pixels. The created mask ensures that only G-neighbor pixels are used to find the average of the frames. Since this mask is updated after each iteration, noise artifacts can be removed almost completely.

B. Proposed Design

Hardware implementation of the proposed method for three consecutive images is demonstrated in Fig. 2a. It consists of a Series in Parallel Out Analog Shift Register (SIPO ASR), Max/Min selector, subtractor, inverter with adjustable threshold and averaging blocks. The input to the ASR is the voltage signal from pixel sensor in range of 0V to 1V.

1) Series in Parallel Out Analog Shift Register: SIPO ASR is built with three functional blocks, as it is shown in Fig. 2b-2d. In the first block, the signal is sampled with a conventional *Sample and Hold* circuit, which consists of NMOS transistor as a switch, a capacitor, and an operational amplifier. The holding duration is $50\mu s$ that translates to a maximum of 20000 frames per second speed. The quantized version of the original signal is then fed to the three parallel connected asynchronously clocked switches: *Switch 1*, *Switch 2* and *Switch 3* together build up the second component. As illustrated in Fig. 2c, each switch is made up of a resistor (R_1, R_2, R_3) and a NMOS transistor with different clocking time (clk_1, clk_2, clk_3) in a voltage divider configuration. Switches are clocked so that the first switch clk_1 is ON when the first sample of the signal arrives from the previous block. The second switch clk_2 is ON when the second sample of the signal arrives. The third switch, respectively, is ON, when the third sample approaches.

In Fig. 2d, the third building block of the ASR is a *Peak detection and Hold* component, that functions as a volatile analog memory for storing the pulses until the last pulse from clk_3 arrives. It consists of an input differential pair, current mirror and an output stage [6]. Assuming a positive voltage is applied, the current through transistor M2 is larger than transistor M1. The current carried by transistor M1 is copied by transistors M3 and M4. The difference in current between M1 and M2 is detected by transistor M5. This current is used to charge capacitor C_1, which was initially discharged. When V_{out} reaches its peak state, both inputs of the differential pair become equal, thus turning OFF transistors M5 and M6. Peak value is saved across capacitor. Switches controlled by V_{r1}, V_{r2}, V_{r3} are clocked synchronously, so that the voltage across the capacitor is discharged at the same time.

2) Max/Min Selector: Once intensities of pixels arriving at each frame are accessible at the same time, the next step is to identify whether they belong to G-neighbor category or not. The comparison between pixels is performed by first finding Max and Min of the voltage levels. Subtraction and thresholding operations are carried out by the subsequent circuit components. Filtering operations like Max and Min can be carried out using an analog rank order filter (ROF) [7]. The ROF with two inputs is implemented as presented in Fig. 2e. Two out of three output voltages of ASR, including V_{out1} and reference voltage V_{out2}, are processed in one ROF block, whereas V_{out3} and V_{out2} are processed in the other block. These voltage pairs are connected to the input branches of differential amplifier, which is biased with a DC current I_3. A tail current source I_4 can be adjusted to select either minimum or maximum rank at the output branch. The relation between I_3 and I_4 is $I_4 = (N-k+2)I_3$, where N is the rank order of ROF and k belongs to range $1 < k < N$. In our case, N=2, and V_{out} selects minimum voltage out of two inputs for k=1 and maximum for k=2. To identify both the minimum and maximum of two voltages in a parallel manner there are two configurations of ROF as in Fig. 2e within one block. I_3 is 5 μA for both cases, whereas I_4 is 10 μA and 15 μA for maximum and minimum voltage selection, respectively.

3) Analog Voltage Subtractor: The distance between pixels in each frame is calculated using an analog voltage subtractor as in Fig. 2f [8]. Subtraction operation is implemented with two pairs of differential amplifiers, where currents I_{s1} and I_{s2} are linearly proportional to $V_{rank1} - V_{diff}$ and $V_{rank2} - V_{offset}$ respectively as demonstrated in (3) and (4).

$$I_{s1} = K(V_{rank1} - V_{diff}) \tag{3}$$

$$I_{s2} = K'(V_{rank2} - V_{offset}) \tag{4}$$

K and K' are constants that depend on the sizing of the transistors and bias currents I_5 and I_6. In the equilibrium state, sum of I_{s1} and I_{s2} must be zero. Assuming two differential pairs are exactly the same, K and K' can be cancelled. This leads to the relation between inputs and output of the subtractor block

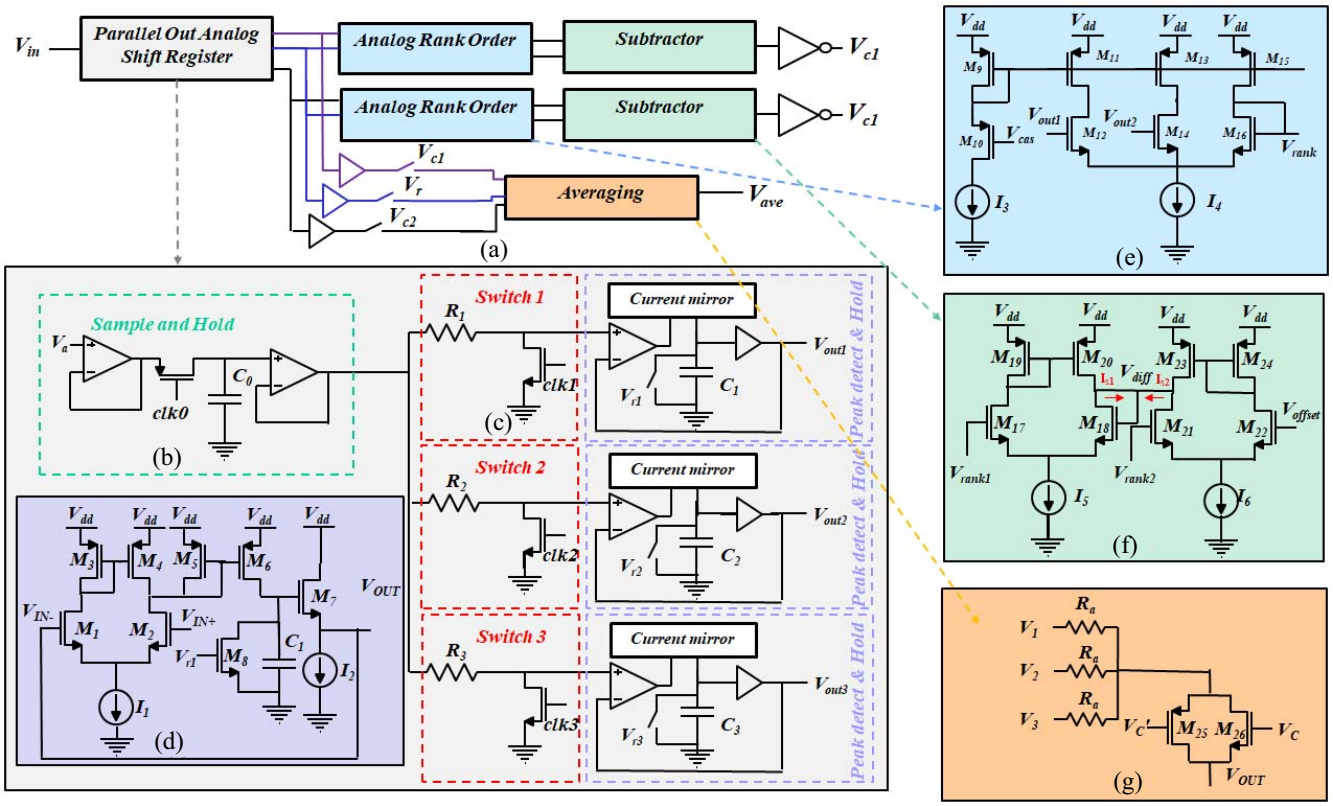

Fig. 2. Hardware implementation of temporal G-neighbor filter.

to be as in (5).

$$V_{diff} = V_{rank1} - V_{rank2} + V_{offset} \tag{5}$$

V_{offset} is set to 0.5V. Calculated distance between V_{rank1} and V_{rank2} is then thresolded using a CMOS inverter. The threshold of the inverter can be adjusted by varying transistor dimensions. The logical '0' (0V) or '1' (1.8V) can be accessed at the output of inverter.

4) Averaging: In Fig. 2g, averaging circuit consists of three identical resistors in parallel, set of switches and buffers. Switches are controlled by voltages (V_{c1}, V_{c2}, V_{c3}), so that only neighboring pixels can be averaged.

III. Results

A. System Simulations

The performance of proposed method is compared to a conventional temporal mean filter. For our simulations, raw videos of Saturn, Jupiter and Mars taken with 10-inch Meade LX200 telescope are used [9]. Salt and pepper noise with variance of 0.5 percent is added to the video. Window size for temporal filtering is selected to be five frames. After running simulations for different window sizes, optimum threshold, η, was found to be 40% of maximum intensity (or threshold corresponds to 0.72V) for all three cases, where the dark pixel corresponds to 0V and white pixel corresponds to a voltage level of 1.8V. In Fig. 3a, original video frames of Saturn are illustrated. Fig. 3b demonstrates implementation of a conventional temporal mean filter for denoising. Similarly, Fig. 3c shows edge detection

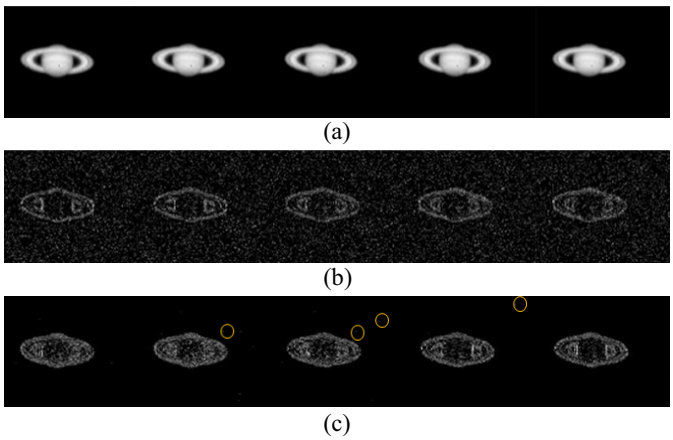

Fig. 3. Comparison of edge detection for (a) video frames with (b) conventional temporal mean filter versus (c) proposed temporal G-neighbor filter.

performed after applying a temporal G-neighbor filter on several frames of the video. The remaining noisy pixels are shown in yellow circles. It can be noticed that edge detection after removing noise artifacts with proposed method exhibits a clear visual enhancement.

We performed a set of simulations to identify the effect of threshold value. Fig. 4 shows a SSIM as a function of similarity threshold versus four different window sizes for a video of Saturn. It can be observed that the SSIM improves with an increase in similarity threshold until it reaches optimum value at 40% of maximum intensity of 1 (or 0.72V). After

TABLE I
IMAGE QUALITY METRICS FOR THREE SAMPLE VIDEOS

Filter	Saturn			Jupiter			Mars		
	MSE	PSNR	SSIM	MSE	PSNR	SSIM	MSE	PSNR	SSIM
Window size = 3									
Mean	0.1361	8.66622	0.1756	0.1638	7.8590	0.1730	0.1379	8.6052	0.1551
Proposed	**0.0136**	**18.7756**	**0.9341**	**0.0635**	**11.9978**	**0.7693**	**0.0101**	**20.0487**	**0.9538**
Window size = 5									
Mean	0.1219	9.1597	0.2901	0.1526	8.1680	0.2670	0.1253	9.0229	0.2693
Proposed	**0.0177**	**17.6438**	**0.9139**	**0.0714**	**11.4621**	**0.7381**	**0.0119**	**19.3088**	**0.9444**

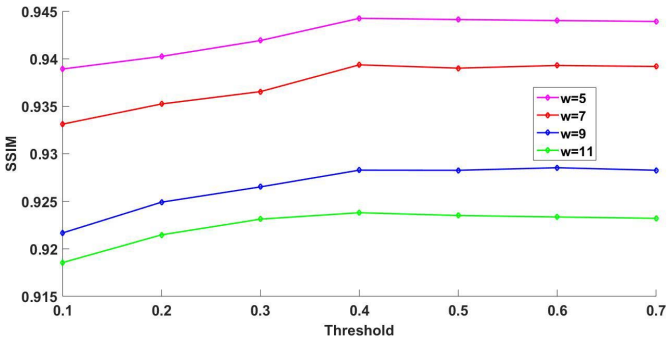

Fig. 4. SSIM versus threshold for four different windows. The thresholds are shown as normalized between 0 and 1, here, 0 (or 0V) represents a dark pixel and 1 (or 1.8V) represents a white pixel.

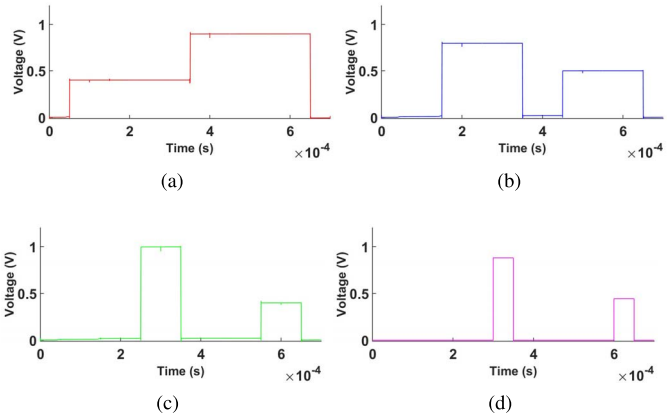

Fig. 5. Three values saved in ASR in parallel: (a) Frame 1 , (b) Frame 2, (c) Frame 3. (d) Response of temporal G-neighbor filter for given values of inputs of 0.4V, 0.8V and 1V in the first cycle and 0.9V, 0.5V and 0.4V in the second cycle.

that, the performance of temporal G-neighbor filter slightly deteriorates. This is due to the fact that a number of falsely selected G-neighbor pixels increases if a high value of the similarity threshold is chosen. The results were consistent with the remaining two sample videos demonstrating the same optimum similarity threshold.

Table I illustrates different image quality metrics that were used to quantify the performance of proposed method against a conventional temporal mean filtering algorithm for edge detection. Mean Square Error (MSE) [10] evaluates the presence of noise, Peak Signal-to-Noise Ratio (PSNR) [11] shows a strength of the signal against corrupting noise, and the Structural Similarity Index Measure (SSIM) [12] defines the similarity between two images similar to human perception. There are noticeable improvement in all three measures. For window size of three, MSE is on average 10, 2.58 and 13.6 times (6.88, 2.14 and 10.5 times for window size of five) lower for the proposed method for videos of Saturn, Jupiter and Mars, respectively.

In astronomical photography, exposure time for recording of images can get from a few hours to days. The image is obtained by stacking several frames of the sequence. The noise on each frame contributes to unwanted defects in the final image, including smudging, blurring or smoothing of edges. Proposed method allows to perform real-time processing of the recording, so that extensive processing of enormous amount of data to remove noise is avoided.

B. Temporal G-Neighbor Filtering

The proposed circuit is simulated for three consecutive frames using TSMC's 180 *nm* CMOS technology. Fig. 5a–5d depicts resulting timing diagrams of SPICE simulation. For demonstration purposes, two cycles of processing are shown. An input to the ASR is signal from the pixel sensor. Three parallel voltage pulses are kept at the output of the ASR. These voltage levels are 0.4V, 0.8V and 1V for first cycle and 0.9V, 0.5V and 0.4V for second cycle as shown in Fig. 5a–5c. In Fig. 5d, the average of second and third voltage intensity levels is calculated. Voltages 0.4V and 0.9V for the first and second cycles respectively are ignored due to the fact that they are not neighbor pixels with the reference frame.

TABLE II
TRANSISTOR SIZING FOR CIRCUITS IN FIG. 2

	Transistors	W/L[1]
ASR	M1-M2	$5\lambda/1.5\lambda$
	M3-M4	$5\lambda/2\lambda$
	M5	$5\lambda/1\lambda$
	M6	$15\lambda/1\lambda$
	M7	$5\lambda/1\lambda$
	M8	$2\lambda/2\lambda$
Analog ROF	M9-M13,M15	$12\lambda/1\lambda$
	M14	$5\lambda/1\lambda$
	M16	$10\lambda/1\lambda$
Subtractor	M17-M18,M21-M22	$8\lambda/5\lambda$
	M19-M20,M23-M24	$5\lambda/5\lambda$
Switches	M25-M26	$1\lambda/1\lambda$

[1] λ corresponds to $180nm$

C. Area and Power Consumption

Table II illustrates transistor aspect ratios for each computation block. Due to their small size and compatibility with CMOS technology, resistors are replaced by memristors [13].

Memristors can be programmed to certain resistive state, and remain there until voltage across positive and negative terminals exceeds a set threshold value. The memristor used for this simulation has physical dimensions of 50 *nm* by 50 *nm* [14]. MOS capacitors for 180 *nm* technology are used.

The total post-layout area of analog pre-processing block for a single pixel for averaging three elements corresponds to 2137 μm^2. Power consumption for supply voltage of 1.8V is on average 1.12 *mW* per cycle. The circuit in Fig. 2 can be further modified to perform an averaging of 5 elements. A number of circuit elements increases for a 5-element averaging. Specifically, there is a need for a single sample-and-hold circuit, 5 peak-detector-and-hold circuit and switching blocks, 4 pairs of Max/Min selectors, 4 subtractors, 5 buffers, 4 inverters and 15 memristors in total. Therefore, total area and power consumption of the circuit for 5 elements is also larger than for 3 elements. For 5-element averaging, post-layout area and power consumption are 2908 μm^2 and 1.88 *mW* per cycle, respectively. This is compatible with existing large CMOS and CCD (Charge Coupled Device) image sensors used for exploring for space and astronomical objects. Their pixel sizes can vary from 15 μm [15] to 70 μm [16], [17].

There are several aspects of circuit design concerned when integrating the temporal G-neighbor filter with the external modules. The filtered image can be processed in the analog or digital domain with additional circuitry. Edge detection is one option, but other operations, such as image segmentation or object recognition, can also be performed. This will require the use of analog-to-digital converters, control and memory units. Furthermore, integration of the filter with the pixel is different in cases where CMOS and CCD sensors are used. In-pixel processing is more common for CMOS image sensors, e.g., in-pixel analog-to-digital converters, whereas analog pre-processing is done externally in CCD image sensors. Additionally, electromagnetic (EM) and temperature analysis of the circuit layout need to be carried out. Integrating with CCD image sensors may require additional cooling to minimize dark current.

IV. Conclusion

In this brief, we proposed a temporal G-neighbor filter to remove impulse noise from astronomical videos. The proposed method, when used for edge detection in the noisy astronomical videos, showed structural preservation of the edge features with noise removal. The improvements are demonstrated by about eight times reduction in MSE, two times increase in PSNR and three times increase in SSIM values. The circuit for G-neighbor filtering for three consecutive frames has been tested with this design. This design can be used as an analog pre-processing unit within or near to the existing large CMOS or CCD image sensors.

The analog domain circuits for feature extraction near a pixel can be a useful topic to explore further for astronomical imaging as the pixel sizes are large allowing to pack larger analog processing circuits within or near to a pixel. At the same time, the analog domain processing also allows to capture high speed events at relatively lower cost in comparison with digital pixels that will require several layers of post-processing to perform at very high sampling rates. Further, the proposed post-processing of signals from pixels in time through analog domain can also help unravel structural changes of moving objects without additional noise removal filters.

References

[1] A. U. Lagies, L. Gohler, J. Sigg, P. Turkes, and R. Kraus, "Degradation modeling of semiconductor devices and electrical circuits," in *Proc. IEEE Int. Conf. Semicond. Electron. (ICSE)*, Nov. 1998, pp. 86–90.

[2] G. R. Hopkinson, C. J. Dale, and P. W. Marshall, "Proton effects in charge-coupled devices," *IEEE Trans. Nucl. Sci.*, vol. 43, no. 2, pp. 614–627, Apr. 1996.

[3] A. Popowicz, A. R. Kurek, T. Blachowicz, V. Orlov, and B. Smolka, "On the efficiency of techniques for the reduction of impulsive noise in astronomical images," *Monthly Notices Roy. Astron. Soc.*, vol. 463, no. 2, pp. 2172–2189, 2016. doi: 10.1093/mnras/stw1983.

[4] P. E. Allen and D. R. Holberg, *CMOS Analog Circuit Design* (The Oxford Series in Electrical and Computer Engineering). New York, NY, USA: Oxford Univ. Press, 1987. [Online]. Available: http://cds.cern.ch/record/2306311

[5] T. E. Boult, R. A. Melter, F. Skorina, and I. Stojmenovic, "G-neighbors," in *Proc. SPIE*, 1993, p. 2060. [Online]. Available: https://doi.org/10.1117/12.165007

[6] F. Borghetti, R. Magni, P. Malcovati, and A. Rossini, "A double polarity CMOS peak-and-hold circuit for satellite radiation detection systems," in *Proc. 12th IEEE Int. Conf. Electron. Circuits Syst.*, Dec. 2005, pp. 1–4.

[7] J. Ramirez-Angulo, R. Gonzalez-Carvajal, G. O. Ducoudray, A. J. Lopez-Martin, and A. Torralba, "New compact CMOS continuous-time low-voltage analog rank-order filter architecture," *IEEE Trans. Circuits Syst. II, Exp. Briefs*, vol. 51, no. 5, pp. 257–261, May 2004.

[8] S. W. Tsay and R. W. Newcomb, "A neural-type pool arithmetic unit," in *Proc. IEEE Int. Symp. Circuits Syst.*, vol. 5, Jun. 1991, pp. 2518–2521.

[9] *Videos of the Planets.* Accessed: Jun. 1, 2018. [Online]. Available: www.skyimaging.com/astronomy-videos.php

[10] R. C. Gonzalez and R. E. Woods, *Digital Image Processing*, 2nd ed. New York, NY, USA: Prentice-Hall, 2002.

[11] Q. Huynh-Thu and M. Ghanbari, "Scope of validity of PSNR in image/video quality assessment," *Electron. Lett.*, vol. 44, no. 13, pp. 800–801, Jan. 2008.

[12] Z. Wang, A. C. Bovik, H. R. Sheikh, and E. P. Simoncelli, "Image quality assessment: From error visibility to structural similarity," *IEEE Trans. Image Process.*, vol. 13, no. 4, pp. 600–612, Apr. 2004.

[13] D. B. Strukov, G. S. Snider, D. R. Stewart, and R. S. Williams, "The missing memristor found," *Nature*, vol. 453, no. 7191, pp. 80–83, 2008.

[14] W. Lu, K.-H. Kim, T. Chang, and S. Gaba, "Two-terminal resistive switches (memristors) for memory and logic applications," in *Proc. 16th Asia South Pac. Design Autom. Conf. (ASPDAC)*, Yokohama, Japan, 2011, pp. 217–223. [Online]. Available: http://dl.acm.org/citation.cfm?id=1950815.1950868

[15] S. E. Holland, D. E. Groom, N. P. Palaio, R. J. Stover, and M. Wei, "Fully depleted, back-illuminated charge-coupled devices fabricated on high-resistivity silicon," *IEEE Trans. Electron Devices*, vol. 50, no. 1, pp. 225–238, Jan. 2003.

[16] P. Jorden, P. Jerram, M. Fryer, and K. Stefanov, "E2V CMOS and CCD sensors and systems for astronomy," *J. Instrum.*, vol. 12, no. 7, 2017, Art. no. C07008.

[17] *CMOS Custom Professional Image Sensors.* Accessed: Jun. 1, 2018. [Online]. Available: www.teledyne-e2v.com/products/imaging/cmos-image-sensors-for-space-and-ground-based-astronomy/